PAPER

Compression of femtosecond pulses in a wide wavelength range using a large-mode-area tapered fiber

IOP Publishing | Astro Ltd Laser Physics
Laser Phys. **29** (2019) 025104 (9pp) https://doi.org/10.1088/1555-6611/aaf63f

Compression of femtosecond pulses in a wide wavelength range using a large-mode-area tapered fiber

M Rehan[1], G Kumar[1], V Rastogi[1], D A Korobko[2] and A A Sysolyatin[2,3]

[1] Department of Physics, Indian Institute of Technology Roorkee, Roorkee 247667, Uttarakhand, India
[2] Ulyanovsk State University, L. Tolstoy Str., 42, 432017 Ulyanovsk, Russia
[3] General Physics Institute, Russian Academy of Sciences, 38 Vavilov Str., 119333, Moscow, Russia

E-mail: rehan.dph2016@iitr.ac.in

Received 23 July 2018, revised 2 October 2018
Accepted for publication 23 November 2018
Published 9 January 2019

Abstract

We report the design of a tapered fiber that can be used for the compression of pulses at different central wavelengths. The proposed fiber is a three-layer W-type large-mode-area fiber, which has been tapered to transform the mode area from 1700 μm^2 to 900 μm^2. We determine the exact length of the maximum pulse compression and numerically demonstrate the compression of a 250 fs, 100 kW peak power input pulse to 15 fs, 850 kW at 1.55 μm wavelength and compression of 250 fs, 120 kW peak power input pulses to 28 fs, 700 kW and to 46 fs, 500 kW at 1.8 μm and 2 μm wavelengths, respectively. Such a fiber can find wide ranging applications, including in communication, spectroscopy and medicine.

Keywords: pulse compression, large-mode-area fiber, pulse shaping, tapered fiber, high peak power femtosecond pulses, ultrafast processes in fiber

(Some figures may appear in colour only in the online journal)

1. Introduction

The generation and propagation of high peak power ultra-short pulses through a short distance of an optical fiber at different wavelengths have potential in a variety of high-power applications [1–4]. For example, high peak power ultra-short pulses, at 1.55 μm wavelength are used in optical communication systems [5], pulses of 1.8 μm wavelength are useful in spectroscopy and laser ablation [6, 7], while pulses at 2 μm wavelength are used in medical treatments [7, 8]. Various investigations demonstrate that these high peak power ultra-short pulses can be generated using fiber lasers and amplifiers but fiber lasers suffer from complexity of the system and commercial feasibility [9]. In addition, nonlinear effects and thermal tolerance limit the output power of the fiber lasers. To overcome these difficulties, the optical pulse compression is another alternative [10–12]. In 1980, Mollenauer *et al* were the first to observe this phenomenon of pulse compression [13]. Later on, they also reported extreme picosecond pulse narrowing by using a soliton effect in single-mode optical fibers [14]. In general, pulse compression is the consequence of the interplay between spectral broadening due to dispersion and self-focusing induced by nonlinear effects [15]. At high power, above the 1.3 μm wavelength, in fused silica fiber, the inherent anomalous dispersion interacts with self-phase modulation (SPM) and leads to the optical compression of the pulse [4]. Pulse compression using axially varying fibers is one of the trending approaches. Axially varying fibers, such as dispersion decreasing fibers, dispersion shifted fibers and tapered fibers, are being used for the purpose of pulse propagation, supercontinuum generation and pulse compression [15–19]. Andrianov *et al* reported the generation of widely tunable few-cycle 20–25 fs short duration pulses in the range of 1.6–2.1 μm by compression of femtosecond pulses using an all-fiber Er-doped laser source [20]. However, they dealt with low peak power femtosecond pulses. Recently, Yuan *et al* proposed an inversely tapered silicon ridge waveguide to compress the picosecond pulses in the mid infrared region [21]. They realized exponential decreasing dispersion along the length of the fiber. The arrangement for the optical pulse

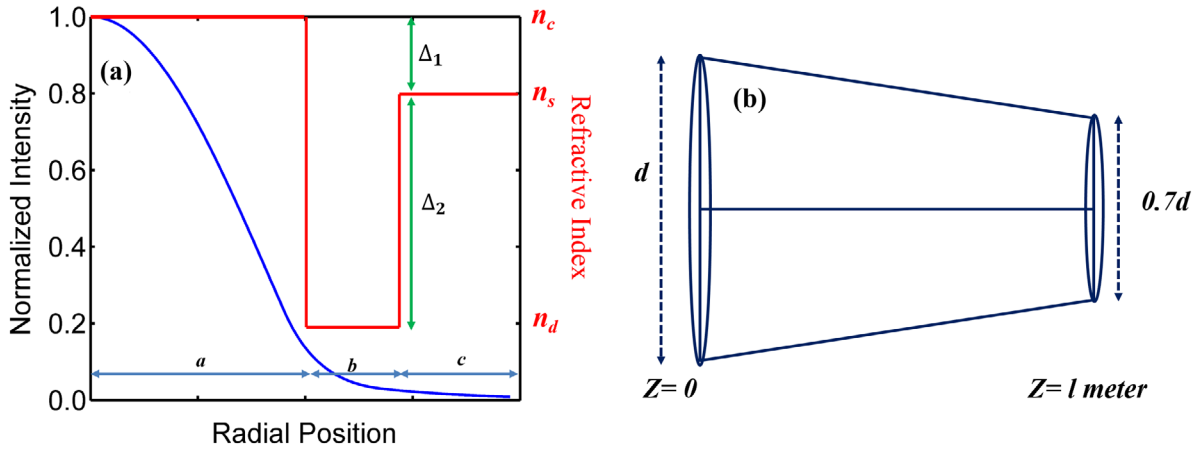

Figure 1. (a) Refractive index profiles of the three-layered structure fiber with the normalized intensity profile of the LP_{01} mode and (b) a schematic of the down-tapered fiber. Here, d and l represent the diameter and length of the fiber, respectively.

compression is simple but necessitates adjusting many parameters, such as the length of the fiber, mode field diameter, input power, input pulse width and dispersion to achieve pulse compression. Gehbhardt *et al* reported the generation of ultra-short pulses of 13 fs duration and 1.4 GW peak power around the 2 μm wavelength from a thulium-doped fiber laser by using a gas filled anti-resonant hollow core fiber [22]. However, this involves handling of the gas filled hollow core fiber. Gaida *et al* reported self-compression of pulses in a solid-core fused silica fiber. They attained pulses of 38 fs duration with an average power of 24.6 W around the 2 μm wavelength [23]. Cardos *et al* reported an Er-doped fiber with a constant core diameter (effective mode area of ~500 μm^2) and achieved ~70 fs pulse with peak power ~120 kW [24]. Nicholson *et al* proposed high peak power amplification of 10 GHz, picosecond and femtosecond pulses in a very-large-mode-area, Er-doped fiber with an effective mode area of ~1100 μm^2 and achieved 130 fs pulses with peak power of 88 kW at the 1.55 μm wavelength [25]. In all these reported works the compression of pulses has only been reported at a single center wavelength, while we have achieved compressed pulses of durations of 15 fs, 28 fs and 46 fs with peak powers of 850 kW, 700 kW and 500 kW at 1.5 μm, 1.8 μm and 2 μm wavelengths, respectively, in a single fiber proposed here.

In this paper, we propose a large-mode-area tapered fiber for optical pulse compression in a wide wavelength range. Our recent work shows direction dependent propagation of femtosecond pulses in a tapered large-mode-area fiber [26]. We study the influence of the mode area variation on the length of the fiber and determine the precise length of the maximum pulse compression at different wavelengths. We numerically demonstrate the compression of a femtosecond Gaussian pulse of 250 fs duration with a peak power of 100 kW at 1.55 μm wavelength through the 40 cm length of fiber and obtain an output pulse of 850 kW peak power with a pulse duration of 15 fs. We show the compression of a 250 fs, 120 kW peak power pulse by using a 30 cm length of the same fiber at 1.8 μm wavelength to 700 kW, 28 fs duration pulses. In addition, we numerically demonstrate compression of a 120 kW, 250 fs Gaussian pulse and achieve 500 kW, 46 fs duration output pulse at 2 μm wavelength. Compression of such high peak power fs pulses of different center wavelengths using the same fiber makes the fiber design versatile and interesting for imaging and material processing applications [27, 28].

2. Fiber design

To accommodate high peak power while maintaining good beam quality, we use a large-mode-area fiber based on higher order mode discrimination [25]. The nonlinear coefficient in a fiber is related to the mode effective area by the following relation

$$\gamma = \frac{\omega_o n_2}{c A_{\text{eff}}} \tag{1}$$

where, γ, ω_o, n_2, c and A_{eff} represent the nonlinear coefficient, central frequency, nonlinear refractive index, speed of light and mode effective area of the fiber, respectively. To satisfy the above-mentioned requirements, we have taken the large-mode-area three-layered structure fiber proposed by Babita *et al* [29] and down-tapered it such that the width ratio of all three layers remains unchanged. Here, the mode area varies from 1700 μm^2 to 900 μm^2 at 1.55 μm wavelength. The normalized intensity and refractive index profiles with radial position and a schematic of the down-tapered fiber are shown in figures 1(a) and (b), respectively. Here, the core of the fiber is made of Ge-doped silica (n_c) and the depressed and outer claddings are F-doped silica (n_d) and pure silica (n_s), respectively. The values of the various parameters are chosen as the core radius (a) = 30 μm, width of the depressed cladding (b) = 15 μm, width of the outermost layer (c) = 17.5 μm, the relative index difference of the core with respect to the outer most silica layer is $\Delta_1 = 0.03\%$, and that of the depressed cladding is $\Delta_2 = 0.08\%$. Here, Δ_1 and Δ_2 are taken such that the fiber supports the LP_{01} and LP_{11} modes only and all the other higher order modes are stripped off. We have used the transfer matrix method (TMM) to analyze the modal characteristics of the fiber [30].

The pulse compression without pulse breaking through such a fiber is obtained by appropriate tapering of the fiber. Tapering of the fiber leads to variations in the effective mode area (A_{eff}) and the effective index (n_{eff}) of the fiber.

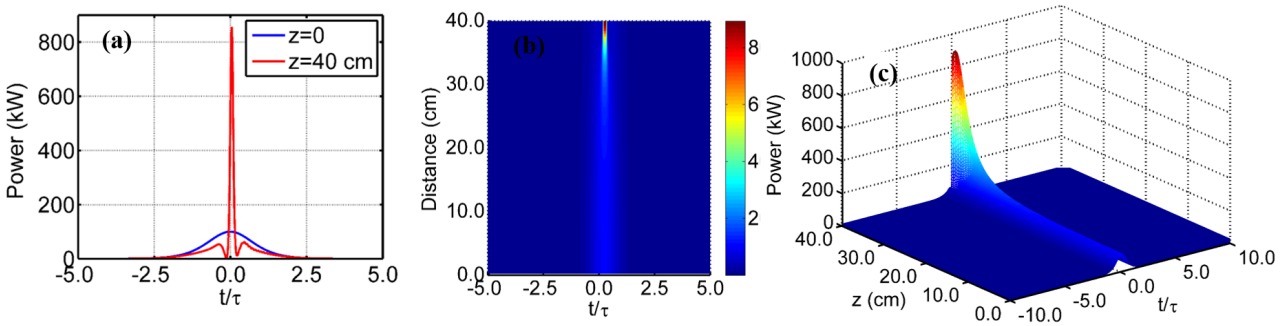

Figure 2. (a) The temporal profiles of the input/output pulses, (b) the corresponding contour plot and (c) the pulse evolution along the 40 cm length of the LMA tapered fiber at 1.55 μm wavelength.

The changes in n_{eff} lead to a change in the dispersion (D). The mathematical form of A_{eff} is given as

$$A_{\text{eff}} = \frac{2\pi\left[\int_0^\infty |\phi_r|^2 r dr\right]^2}{\int_0^\infty |\phi_r|^4 r dr}. \tag{2}$$

And the dispersion coefficient is given by

$$D = -\frac{\lambda}{c}\frac{\partial^2 n_{\text{eff}}}{\partial \lambda^2} \tag{3}$$

where, $\phi_r(r)$, c and λ represent the radial part of the field, the speed of light and the central wavelength, respectively. Hence, dispersion and nonlinearity vary along the length of the fiber with this axial variation, i.e. tapering of the fiber. This tapering reduces the mode area over the length of the fiber and increases the nonlinearity without significantly affecting the dispersion. This leads to compression of the pulses.

3. Theory

To realize the propagation of ultra-short pulses of high peak power through the optical fiber, it is important to include dispersion, nonlinear effects and losses in the fiber. The equation which governs the aforementioned propagation of pulses through the optical fiber is the nonlinear Schrodinger equation (NLSE) [4, 31].

$$\frac{\partial A(t,\, z)}{\partial z} = \left(-i\frac{\beta_2}{2}\frac{\partial^2}{\partial T^2} + \frac{\beta_3}{6}\frac{\partial^2}{\partial T^2} - \frac{\alpha}{2} + i\gamma\left(|A|^2 + \frac{i}{\omega_0}\frac{1}{A}\frac{\partial}{\partial T}\left(|A|^2 A\right) - T_R\frac{\partial |A|^2}{\partial T}\right)\right)A \tag{4}$$

where, A $(t,\, z)$ represents the slowly varying envelope of the pulse amplitude and α is the loss coefficient of the fiber. The parameters ω_o and T_R are the central frequency and Raman time constant. Here, β_2 and β_3 are the dispersions of the second and third order, respectively, while T represents the scaled time, which is given by

$$T = t - \frac{z}{v_g}. \tag{5}$$

The second order dispersion is given by

$$\beta_2 = -D\frac{\lambda^2}{2\pi c} \tag{6}$$

where, v_g and D represent the group velocity of the pulse envelope and dispersion coefficient, respectively. On tapering the fiber, D varies along the length of the fiber. Hence, the second order dispersion coefficient β_2 also changes, accordingly. The variation of the third order dispersion coefficient β_3 is very small so that we have chosen the constant values of 0.104 ps^3 km^{-1}, 0.157 ps^3 km^{-1} and 0.149 ps^3 km^{-1} at the wavelengths 1.55 μm, 1.8 μm and 2 μm, respectively. We have used the split-step Fourier method (SSFM) to solve the above NLSE [4]. Here, we have tapered the fiber to optimize nonlinearity and dispersion in order to achieve pulse compression.

4. Results and discussion

We have studied the propagation of a femtosecond Gaussian pulse through the proposed large-mode-area (LMA) tapered fiber. The mathematical form of the input pulse is given by

$$A\,(\,t,\, z = 0) = A_o \exp(-t^2/2t_0^2) \tag{7}$$

where $A_o(=\sqrt{P_o})$ represents the pulse amplitude, P_o stands for the input power and t_o is the input pulse width. We have down-tapered the fiber and optimized the input parameters in such a way that nonlinear effects, mainly SPM, dominate over dispersion and pulse compression is achieved. In our study the effect of stimulated Raman scattering (SRS) is negligible, since the femtosecond pulses and the generally Raman vibrations are also in the order of hundreds of femtoseconds [32, 33]. Aside from this, the effective mode area of our fiber is in the order of 10^3 μm^2, which increases the Raman threshold [4].

4.1. Pulse compression at 1.55 μm wavelength

To demonstrate the compression of the Gaussian pulse at 1.55 μm, we have solved the NLSE for propagation of an input pulse of 250 fs duration with peak power of 100 kW through a 40 cm length of the proposed fiber. This length corresponds to

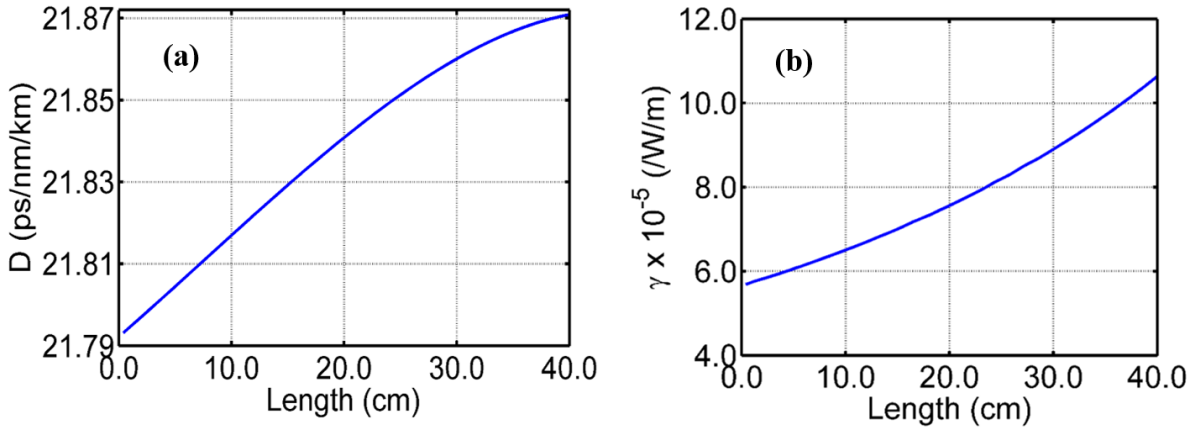

Figure 3. Variation of (a) the dispersion coefficient (D), and (b) the nonlinear coefficient (γ) with the length of the fiber at 1.55 μm wavelength.

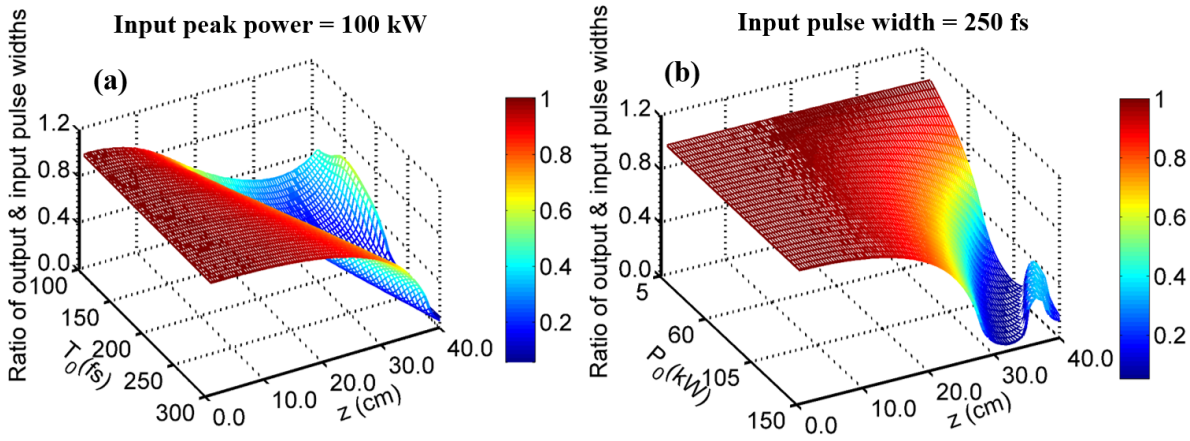

Figure 4. The ratio of the output and input pulse widths with a 40 cm length of the fiber, for (a) pulse widths varying from 100 fs to 300 fs with peak power of 100 kW, (b) peak power is varied from 5 kW to 150 kW while keeping the pulse width 250 fs. Here, T_0, P_0 and z represent the input pulse width, input peak power and length of the fiber.

the maximum achievable compression and has been optimized by calculating the pulse widths at various lengths of the fiber. The temporal shapes of the input and output pulses are shown in figure 2(a) by the blue and red colors, respectively, which clearly shows the compression of the pulse. The peak power of the output pulse is 850 kW and the pulse duration is 15 fs.

A compression factor of approximately 17 has been obtained. The corresponding contour plot and the pulse evolution along the length of the fiber are shown in figures 2(b) and (c), respectively.

To understand the underlying physics, the dispersion (D) and nonlinear coefficients (γ) have been plotted with the length of the fiber in figures 3(a) and (b), respectively. Figures 3(a) and (b) show that the dispersion and nonlinear coefficient are increasing along the length of the fiber but the increase in the nonlinear coefficient is larger than that in the dispersion. Consequently, SPM dominates over group velocity dispersion (GVD) along the length of the fiber and compression of the pulse observed. There are various parameters such as input pulse width, input peak power, fiber length and dispersion that need to be optimized to achieve the optical pulse compression. For the chosen fiber parameters, the pulse width has been varied for a constant input peak power to obtain the maximum compression of the optical pulse. Similarly, for a constant input pulse width the input peak power has been varied to optimize the peak power of the input pulse.

4.2. Effect of the input pulse width and peak power

The pulse width of the input pulse has been varied from 100 fs to 300 fs in steps of 5 fs and the pulse propagation over the maximum achievable pulse compression length (40 cm) of the LMA tapered fiber has been studied.

The input peak power has been chosen as 100 kW. The ratio of output to input pulse widths has been plotted with respect to the length of the fiber, as shown in figure 4(a). The plot shows the pulse compression for the chosen range of pulse width. The compression of the pulse increases with the increase in the input pulse width and the maximum compression of the pulse has been observed around the 250 fs pulse width. Hence, we have chosen the value of the pulse width as 250 fs for our further calculations.

In a similar way, we have fixed the value of the input pulse width as 250 fs and varied the peak power of the input pulse from 5 kW to 150 kW for a 40 cm length of the proposed fiber. We have plotted the ratio of output to input full width at half

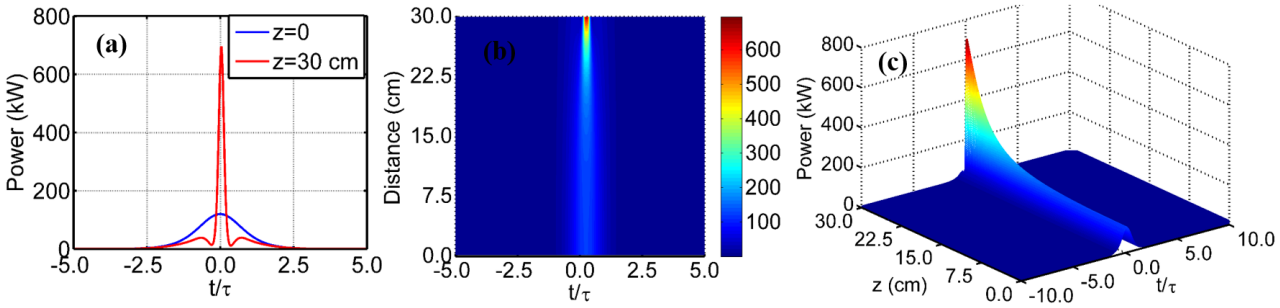

Figure 5. (a) The temporal profiles of the input/output pulses, (b) the corresponding contour plot and (c) the pulse evolution along the 30 cm length of the LMA tapered fiber at 1.8 μm wavelength.

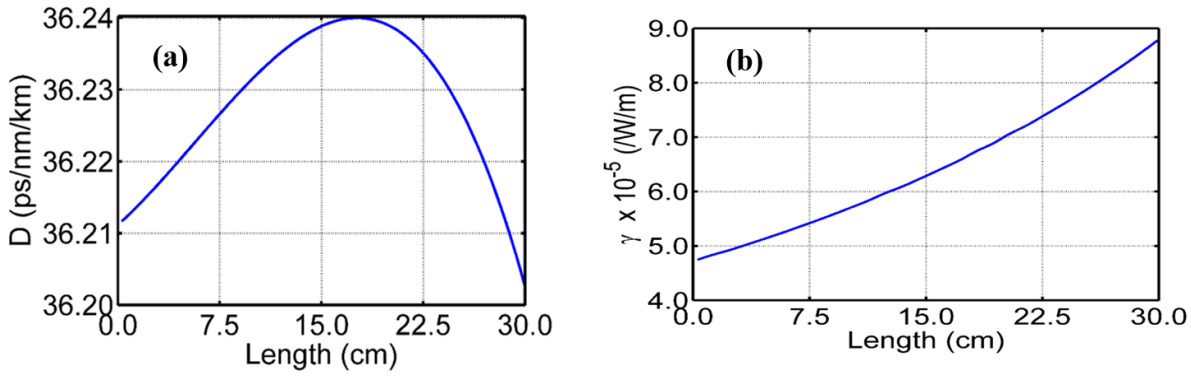

Figure 6. Variation of (a) the dispersion coefficient (D), and (b) the nonlinear coefficient (γ) with the length of the fiber at 1.8 μm wavelength.

maximum (FWHM) with the length of the fiber for different values of input peak powers, as shown in figure 4(b). It has been observed that with the increase in the peak power, the pulse compression increases and the maximum compression is achieved at 100 kW. On further increase in peak power, the pulse compresses up to 30 cm of the length and beyond that it starts dispersing periodically.

4.3. Pulse compression at 1.8 μm wavelength

Ultra-short pulses with high peak power around the 1.8 μm wavelength can be used in spectroscopy [2, 4]. When an ultra-short Gaussian pulse of 250 fs pulse width with 120 kW peak power propagates through the maximum achievable pulse compression length (30 cm) of the proposed fiber, the pulse has been compressed to 28 fs, 700 kW. The corresponding input–output (blue–red) pulses are shown in figure 5(a).

Here, the compression of the pulse can be seen clearly. A compression factor of 9 has been obtained. The contour plot and the pulse evolution through the length of the fiber are shown in figures 5(b) and (c), respectively. The results show that the SPM dominates the GVD along the length of the fiber. This can be understood by looking at the variation in dispersion and the nonlinear coefficient with the length of the fiber, as plotted in figures 6(a) and (b). The plot of dispersion shows that the dispersion coefficient increases up to 17 cm in the length and then decreases drastically for the remaining length of the fiber. In contrast, the plot of the nonlinear coefficient increases throughout the length of the fiber. Hence, SPM dominates over GVD and the compression of the pulse is observed along the length of the fiber.

When comparing figures 3 and 6, it can be clearly seen that the value of the dispersion coefficient is higher in the 1.8 μm wavelength while the nonlinear coefficient is lower in the 1.8 μm wavelength. Hence, the strength of dominance of SPM over GVD is lower in the 1.8 μm wavelength. Therefore, the pulse compression factor is lower but the achieved compression of the pulses is reasonable for use in high-power laser applications. While keeping the peak power constant, we have varied the width of the input pulse to find its maximum compression value. Similarly, we have fixed the input pulse width and varied the input peak power.

4.4. Effect of the input pulse width and peak power

For 120 kW chosen value of the input peak power, we have varied the input pulse width from 100 fs to 300 fs and the pulse propagation over the maximum achievable pulse compression length (30 cm) of the proposed LMA tapered fiber has been studied. For different values of the pulse width, the ratio of the output and input pulse widths with the length of the fiber is shown in figure 7(a).

This shows, on increasing the input pulse width, that compression of the pulse increases and the maximum compression of the pulse has been observed for 250 fs input pulse duration. For 250 fs pulse duration, we have varied the input peak power from 5 kW to 150 kW for the same length of fiber and the ratio of the output and input pulse widths

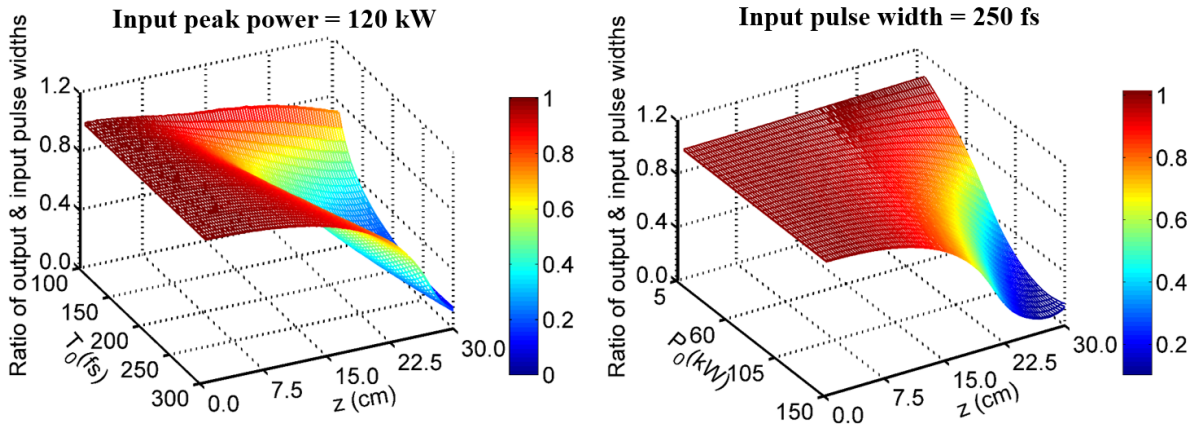

Figure 7. The ratio of output to input FWHM with 30 cm length of the fiber, for (a) a pulse width of 100 fs to 300 fs with constant 120 kW peak power, (b) peak power is varied from 5 kW to 150 kW with 250 fs fixed pulse duration. Here, T_0, P_0 and z represent the input pulse width, input peak power and length of the fiber.

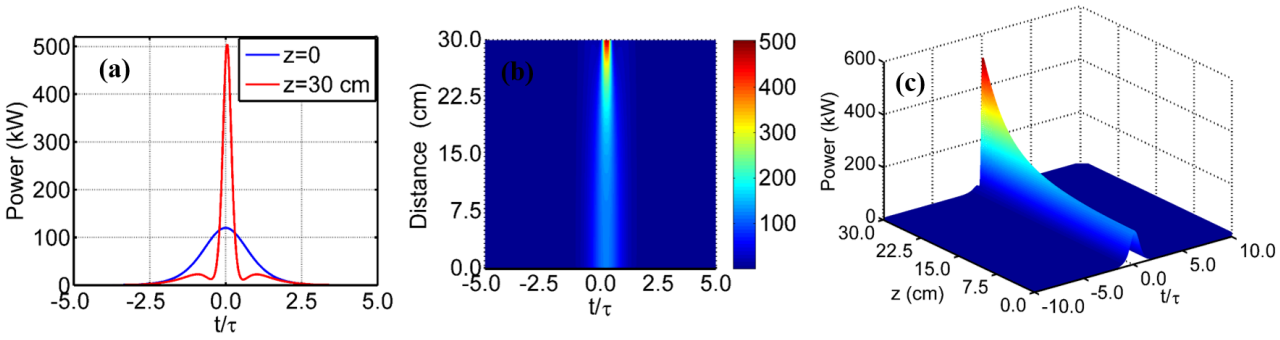

Figure 8. (a) The temporal profiles of the input/output pulses, (b) the corresponding contour plot and (c) the pulse evolution along the 30 cm length of the LMA tapered fiber at 2 μm wavelength.

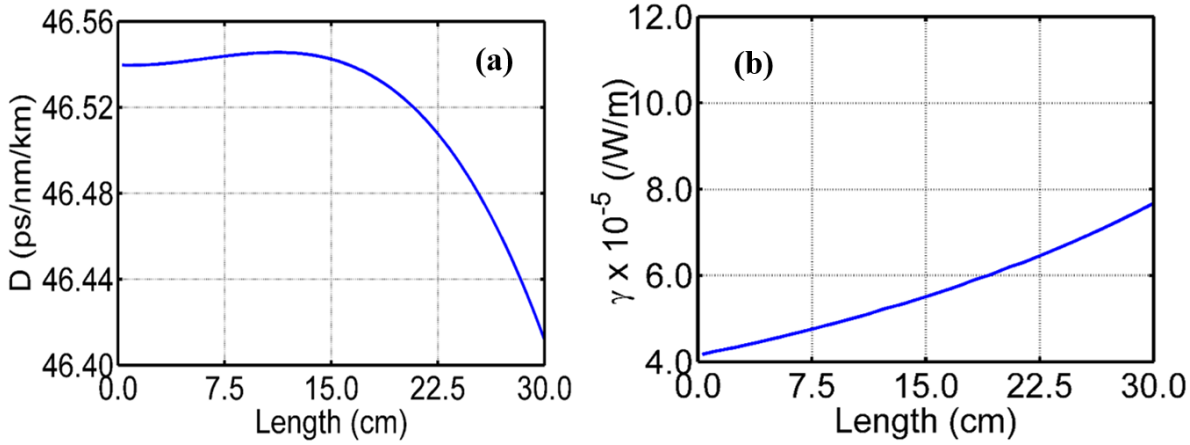

Figure 9. Variation of (a) dispersion, and (b) nonlinear coefficients with the length of the fiber at 2 μm wavelength.

with respect to the length of the fiber is shown in figure 7(b). It can be seen that, for an input peak power around 5 kW, the output pulse is similar to that of the input: while with a further increase in the input peak power, pulse compression is observed. The maximum pulse compression has been achieved around 120 kW input peak power due to dominance of SPM over GVD.

4.5. Pulse compression at 2 μm wavelength

Ultra-short pulses of high peak power at the 2 μm wavelength are useful in high-power medical applications [3]. We have studied the propagation of an input Gaussian pulse of 250 fs duration with peak power of 120 kW through the maximum achievable pulse compression length (30 cm) of the proposed

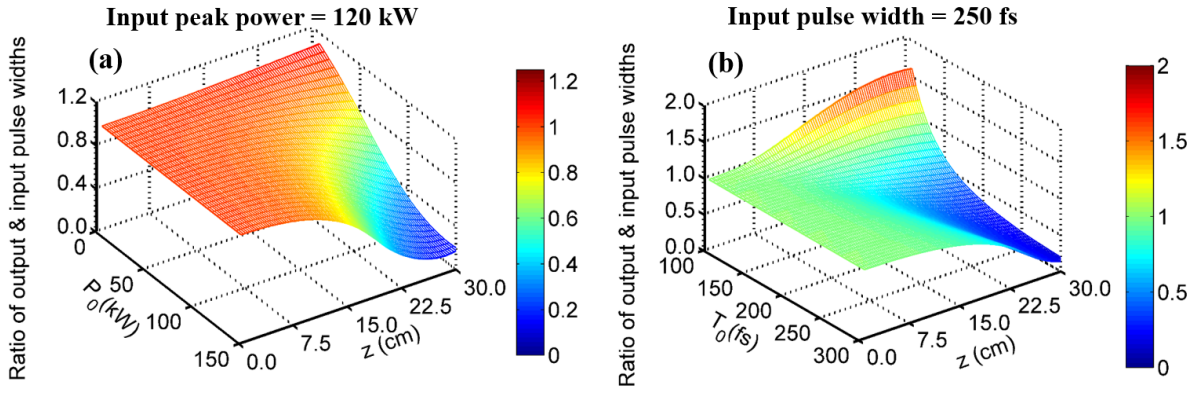

Figure 10. The ratio of output to input FWHM with the 30 cm length of the fiber, for (a) a pulse width of 100 fs to 300 fs with constant 120 kW peak power, (b) peak power is varied from 5 kW to 150 kW with 250 fs fixed pulse duration. Here, T_0, P_0, and z represent the input pulse width, input peak power and length of the fiber.

Table 1. A comparison between down-tapered and uniform (non-tapered) LMA fibers.

			Down-tapered LMA fiber			Uniform (non-tapered) LMA fiber		
Center wavelength (nm)	Input peak power (kW)	Input pulse width (fs)	Length of maximum compression (cm)	Output pulse width (fs)	Peak power (kW)	Length of maximum compression (cm)	Output pulse width (fs)	Peak power (kW)
1550	100	250	40	15	850	65	24	695
1800	120	250	30	28	700	55	42	600
2000	120	250	30	46	500	60	65	420

LMA tapered fiber. A pulse of 500 kW peak power and 46 fs duration is obtained. The pulse width of the output pulse reduced approximately six times compared to that of the input pulse. The temporal shapes of the input and output pulses, the contour plot and the pulse evolution over the length of the fiber are shown in figures 8(a)–(c).

The three-layered structure LMA fiber has been down-tapered so that the dispersion and nonlinear coefficients vary along the length of the fiber, as shown in figures 9(a) and (b). The plots show that the dispersion coefficient is almost constant up to 15 cm of the length and then starts decreasing along the length of the fiber, and the nonlinearity increases along the length of the fiber. Hence, pulse compression is observed due to the interplay between SPM and GVD.

From figures 3, 6 and 9, it can be clearly observed that the value of the dispersion coefficient is higher at a longer wavelength and the case is reversed for the nonlinear coefficient. The strength of the nonlinearity is greater at the 1.55 μm wavelength. Also, the loss coefficient (α) is 0.2 dB km^{-1} at the 1.55 μm wavelength and thus is smaller than that of 1.3 dB km^{-1} and 2 dB km^{-1} at 1.8 μm and 2 μm wavelengths, respectively, for fused silica glass fiber [34]. Therefore, the compression factor is maximum at 1.55 μm, then for 1.8 μm and after that for 2 μm wavelength. The deterioration of pulse compression with increasing center wavelength is due to that fact that as the wavelength increases, there is less confinement of light in the fiber, which results in decreased nonlinearity. The second order dispersion coefficient also increases with the center wavelength. This also leads to broadening of the pulse. Consequently, pulse compression deteriorates with the increase in the wavelength. The input parameters, such as the input pulse width and input peak power, need to be optimized to obtain a significant optical pulse compression.

4.6. Effect of the input pulse width and peak power

The input pulse duration has been varied from 100 fs to 300 fs and the pulse propagation over maximum achievable pulse compression length (30 cm) of the proposed LMA tapered fiber has been studied for a chosen value of 120 kW input peak power. For the selected range of the input pulse width, the ratio of the output and input pulse widths has been plotted with respect to the length of the fiber, which is shown in figure 10(a). We have observed dispersion of the pulse for the input pulse width around 100 fs, while when increasing the input pulse width, a pulse similar to the input is realized. On further increase in the input pulse width, compression of the pulse is attained. We have observed maximum pulse compression around 250 fs input pulse width. Similarly, we have varied the input peak power from 5 kW to 150 kW for the 250 fs input pulse width in the 30 cm length of the fiber and plotted the ratio of the output and input pulse widths with the length of the fiber for all the values of the input peak power, as shown in figure 10(b).

It is observed that the ratio of the output and input pulse widths is lower around 150 kW and lowest at 120 kW input peak power due to dominance of SPM over GVD. Hence, the chosen value of the input peak power for the best compression is 120 kW for our further calculations.

We have also compared the performance of the proposed down-tapered fiber with a uniform fiber. The comparison of a uniform fiber, having parameters $a = 30$ μm, $b = 15$ μm,

$c = 17.5$ μm, $\Delta_1 = 0.03\%$ and $\Delta_2 = 0.08\%$, with the proposed down-tapered fiber is given in table 1. It can be clearly seen that the down-tapered fiber outperforms the uniform fiber in terms of pulse compression and peak powers. The lengths of the maximum compression in the uniform fiber are longer. For example, the maximum compression factor in the uniform fiber is 10 for a 65 cm long fiber, while that in the down-tapered fiber is 17 for a 40 cm length of the fiber at 1.55 μm center wavelength. The pulse compression is improved in the down-tapered LMA fiber. In addition, the down-tapered fiber has an added advantage of sustaining the pulse only in one direction and, thus, avoiding back reflections, which we have already reported in our earlier work [26]. Even though pulse compression can be achieved with standard uniform fibers having small effective mode area, accommodating very high peak powers in these fibers becomes difficult.

5. Conclusion

We have proposed a new design for a three-layer W-type structure large-mode-area down-tapered fiber and numerically demonstrated compression of a 250 fs duration pulse at different wavelengths by means of the same fiber. The exact length of the maximum pulse compression is determined and the influence of the mode area variation with the length of the fiber has been studied. For a 1.55 μm wavelength, a 250 fs, 100 kW pulse compressed to 15 fs, 850 kW while propagated over a 40 cm length of the proposed fiber. These ultra-short pulses can be utilized in ultra-high data rate optical communications. For a 1.8 μm wavelength, a 250 fs, 120 kW pulse was compressed to be 28 fs, 700 kW while transmitted from a 30 cm length of the proposed tapered fiber. For a 2 μm wavelength, a pulse of 250 fs, 120 kW became 46 fs, 500 kW while delivered through 30 cm length of the tapered fiber. These pulses in the eye safe region can be used in spectroscopy, remote sensing and medical treatments. Hence, our fiber design can be a good candidate to produce high peak power ultra-short pulses in a wide wavelength range for a number of high-power applications.

Acknowledgment

This work has been partially supported through the Department of Science and Technology, New Delhi and the Russian Science Foundation (DST-RSF) by an Indo-Russian project on ‘Research and development of new optical fibers for applications in modern laser systems’.

References

[1] Keiffer J C, Fourmox S and Krol A 2017 The ultra-fast high peak power laser in future biomedical and x-ray imaging *Proc. SPIE* **10266** 1026612–8
[2] Decaire I, Jukna V, Paraz C, Millon C, Summerrer L and Couirian A 2016 Spaceborne laser filamentation for atmospheric remote sensing *Laser Photonics Rev.* **10** 481–93
[3] Holzwarth R, Udem T, Hänsch T W, Knight J C, Wadsworth W J and Russell P S J 2000 Optical frequency synthesizer for precision spectroscopy *Phys. Rev. Lett.* **85** 2264–7
[4] Agarwal G P 2013 *Nonlinear Fiber Optics* (New York: Academic)
[5] Nakajima K, Sillard P, Richardson D, Li M J, Essiambre R J and Matsuo S 2015 Transmission media for an SDM-based optical communication system *IEEE Commun. Mag.* **53** 44–51
[6] Elahi P, Akçaalan Ö, Ertek C, Eken K, Ilday F Ö and Kalaycoglu H 2018 High-power Yb-based all-fiber laser delivering 300 fs pulses for high-speed ablation-cooled material removal *Opt. Lett.* **43** 535
[7] Gassino R, Liu Y, Konstantaki M, Vallan A, Pissadakis S and Perrone G 2017 A fiber optic probe for tumor laser ablation with integrated temperature measurement capability *J. Lightwave Technol.* **35** 3447–54
[8] Jackson S D 2009 The spectroscopic and energy transfer characterstics of the rare earth ions used for silicate glass fibre lasers operating in the shortwave infrared *Laser Photonics Rev.* **3** 466–82
[9] Limpert J, Roser F, Schreiber T and Tunnermann A 2006 High-power ultrafast fiber laser systems *IEEE J. Sel. Top. Quantum Electron.* **12** 233–44
[10] Nisoli M, De Silvestri S, Svelto O, Szipöcs R, Ferencz K, Spielmann C, Sartania S and Krausz F 1997 Compression of high-energy laser pulses below 5 fs *Opt. Lett.* **22** 522–5
[11] Fu L, Fuerbach A, Littler I C M and Eggleton B J 2006 Efficient optical pulse compression using chalcogenide single-mode fibers *Appl. Phys. Lett.* **88** 81116
[12] Lassonde P, Mironov S, Fourmaux S, Payeur S, Khazanov E, Sergeev A, Kieffer J C and Mourou G 2016 High energy femtosecond pulse compression *Laser Phys. Lett.* **13** 75401
[13] Mollenauer L F, Stolen R H and Gordon J P 1980 Experimental observation of picosecond pulse narrowing and solitons in optical fibers *Phys. Rev. Lett.* **45** 1095–8
[14] Mollenauer L, Tomlinson W, Stolen R and Gordon J 1983 Extreme picosecond pulse narrowing by means of soliton effect in single-mode optical fibers *Opt. Lett.* **8** 289–91
[15] Korobko D A, Okhotnikov O G, Stoliarov D A, Sysoliatin A A and Zolotovskii I O 2015 Highly nonlinear dispersion increasing fiber for femtosecond pulse generation *J. Lightwave Technol.* **33** 3643–8
[16] Li Q and Huang H 2015 Effective pulse compression in dispersion decreasing and nonlinearity increasing fibers *Opt. Commun.* **342** 36–43
[17] Lavdas S, Driscoll J B, Grote R R, Osgood R M and Panoiu N C 2013 Soliton pulse compression in adiabatically tapered silicon photonic wires *Opt. Express* **22** 6296–312
[18] Manimegalai A, Senthilnathan K, Nakkeeran K and Babu P R 2016 Tapering photonic crystal fibers for generating self-similar ultrashort pulses at 1550 nm *Opt. Eng.* **55** 67108
[19] Korobko D A, Okhotnikov O G, Stoliarov D A, Sysoliatin A A and Zolotovskii I O 2015 Broadband infrared continuum generation in dispersion shifted tapered fiber *J. Opt. Soc. Am.* B **32** 692–700
[20] Andrianov A, Kim A, Muraviov S and Sysoliatin A 2009 Wavelength-tunable few-cycle optical pulses directly from an all-fiber Er-doped laser set-up *Opt. Lett.* **34** 3193–5
[21] Yuan J *et al* 2017 Mid-infrared self-similar compression of picosecond pulse in an inversely tapered silicon ridge waveguide *Opt. Express* **25** 33439–50
[22] Gebhardt M *et al* 2017 Nonlinear pulse compression to 43 W GW-class few-cycle pulses at 2 μm wavelength *Opt. Lett.* **42** 4179–82
[23] Gaida C, Gebhardt M, Stutzki F, Jauregui C, Limpert J and Tünnermann A 2015 Self-compression in a solid fiber to 24

MW peak power with few-cycle pulses at 2 μm wavelength *Opt. Lett.* **40** 5160–3
[24] Cadroas P *et al* 2017 All-fiber femtosecond laser providing 9 nJ, 50 MHz pulses at 1650 nm for three-photon microscopy *J. Opt.* **19** 065506
[25] Nicholson J W, Ahmad R, Desantolo A and Varallyay Z 2017 High average power, 10 GHz pulses from a very-large-mode-area, Er-doped fiber amplifier *J. Opt. Soc. Am.* B **34** A1–6
[26] Kumar G, Rehan M, Rastogi V, Korobko D A and Sysoliatin A A 2018 Direction-dependent propagation of high-power femtosecond pulses through large-mode-area tapered fiber *J. Opt. Soc. Am.* B **35** 1–6
[27] Farrar M J, Wise F W, Fetcho J R and Schaffer C B 2011 *In vivo* imaging of Myelin in the vertebrate central nervous system using third order harmonic generation microscopy *Biophys. J.* **100** 1362–71
[28] Kerse C *et al* 2016 Ablation-cooled material removal with ultrafast bursts of pulses *Nature* **537** 84–9
[29] Hooda B, Rastogi V and Kumar A 2013 Design of large-mode-area three layered fiber structure for femtosecond laser pulse delivery *Opt. Commun.* **293** 108–12
[30] Rastogi V and Chiang K S 2004 Radial-effective-index method *J. Opt. Soc. Am.* B **21** 258–65
[31] Wai P K A, Menyuk C R, Lee Y C and Chen H H 1986 Nonlinear pulse propagation in the neighborhood of the zero-dispersion wavelength of monomode optical fibers *Opt. Lett.* **11** 464–6
[32] O'Donnell M D *et al* 2007 Tellurite and fluorotellurite glasses for fiberoptic Raman amplifiers: glass characterization, optical properties, Raman gain, preliminary fiberization, and fiber characterization *J. Am. Ceram. Soc.* **90** 1448–57
[33] Stolen R H, Gordon J P, Tomlinson W J and Haus H A 1989 Raman response function of silica–core fibers *J. Opt. Soc. Am.* B **6** 1159–66
[34] Miya T, Terunuma Y, Hosaka T and Miyashita T 1979 Ultimate low-loss single-mode fiber at 1.55 μm *Electron. Lett.* **15** 106–8